Through Space Coupling and Fermi Resonances in Neopentane-d_0, -d_6, -d_9, and Tetramethylsilane

Michael W. P. Petryk and Bryan R. Henry*

Department of Chemistry and Biochemistry, University of Guelph, Guelph, Ontario N1G 2W1, Canada

Received: April 10, 2002; In Final Form: July 15, 2002

A comparison of the CH vibrational overtone spectra of vapor phase neopentane-d_0 ($C(CH_3)_4$), -d_6 ($C(CH_3)_2(CD_3)_2$), and -d_9 ($C(CH_3)(CD_3)_3$) and tetramethylsilane (TMS) in the frequency range $\Delta\upsilon_{CH} = 4-8$ (10 800−18 200 cm^{-1}) has revealed pronounced differences between the spectra of TMS and the neopentanes, and subtle differences among the spectra of the neopentanes. These spectral differences are interpreted as a manifestation of geometry and vibrational frequency dependent differences in coupling efficiencies that facilitate the de-excitation of local modes of vibration via IVR. Fermi resonance plays a key role in this coupling. Some of the states are perturbed by *through space coupling* (a collision-like van der Waals interaction) that can facilitate IVR. The normal modes of vibration, which are implicated in Fermi resonance of the neopentanes and TMS, have been calculated ab initio using density functional theory and are shown to be affected by through space interactions.

Introduction

The vibrational overtone stretching transitions of XH bonds (X = C, N, O, etc.) are dominated by transitions to states whose components have all of the vibrational energy localized within one of a set of equivalent XH oscillators. The localization of energy within local modes[1−5] of XH vibrational motion makes overtone spectroscopy an extremely sensitive probe for detecting small changes in the properties of XH bonds, such as bond lengths,[6−8] energy flows in intramolecular vibrational energy redistribution (IVR),[9,10] and conformations.[11,12] In particular, it is possible to use overtone spectroscopy to probe how molecular geometry, normal modes of vibration, and the amplitudes of local XH vibrational modes affect resonances, couplings, and the rate of IVR.

The molecular Hamiltonian, when represented in a local mode basis, contains XH stretch terms for which off-diagonal coupling elements are small compared to the (anharmonic) diagonal cubic and quartic terms.[13] The contributions of the diagonal terms become increasingly dominant, compared to those of the off-diagonal terms, with increasing vibrational excitation. It becomes possible to treat the potential of a molecule with a number of anharmonic oscillators as effectively separable along local modes of vibration. The local mode description has been extended to multioscillator systems in the harmonically coupled anharmonic oscillator (HCAO) model.[5,14−16] It is convenient to treat a molecular potential as a collection of diatomic Morse potentials in which couplings are taken as perturbations because the wave functions of a Morse oscillator can be solved analytically.[9]

The basis states for a series of n equivalent XH Morse oscillators can be written as a product of individual one-dimensional Morse wave functions $|\upsilon_1\rangle|\upsilon_2\rangle...|\upsilon_i\rangle...|\upsilon_n\rangle$ or simply as $|\upsilon_1, \upsilon_2, ..., \upsilon_i, ..., \upsilon_n\rangle$, where υ_i is the number of vibrational quanta in the ith XH oscillator. For higher vibrational overtones ($\Delta\upsilon_{CH} \geq 4$) spectrally "bright" states, i.e., those states that carry intensity from the $\upsilon = 0$ vibrational state, are almost exclusively pure local mode states that can be described by a linear combination of components in which all of the vibrational energy is localized ($|\upsilon, 0, ..., 0\rangle$, $|0, \upsilon, ..., 0\rangle$, etc.). The pure local mode wave functions of three coupled, identical XH oscillators of local $C_{3\upsilon}$ symmetry arising from the linear combination of these basis states may be denoted as $|\upsilon, 0, 0\rangle_{A_1}$ and $|\upsilon, 0, 0\rangle_E$ (the pure local mode wave function of A_2 symmetry carries no intensity). The symmetrized wave functions become increasingly degenerate with increasing excitation so that symmetry effects are generally not observed at $\Delta\upsilon_{CH} \geq 3$ for large molecules such as the neopentanes and TMS. Nearly degenerate states of $C_{3\upsilon}$ symmetry that cannot be resolved from one another can be collectively denoted as $|\upsilon, 0, 0\rangle_{A_1E}$.

The vibrational overtones of gas- and liquid-phase neopentane-d_0, -d_6, and -d_9 and tetramethylsilane (TMS) have been studied with a variety of spectroscopic techniques (see ref 17 and references therein). In this work we will extend the range of a previous study of vapor phase neopentane[18] and its d_6 and d_9 isomers. Photoacoustic (PA) detection gives improved signal-to-noise ratios and allows comparisons between subtle differences in spectral structure. In the absence of coupling to other modes the local mode model predicts that the CH vibrational overtone spectra of neopentane-d_0, -d_6, and -d_9 will be simple, with only one transition peak at each overtone. In fact, the overtone transitions of neopentane have complicated structures that differ between the deuterated isomers. Moreover, the full width at half-maximum (fwhm) values of the CH overtone transitions are larger in the neopentanes than in other $M(CH_3)_4$ homologues (M = Si, Sn, and Ge).[17,19−21] In this paper we attempt to understand the implications of the rich and broad neopentane spectra in terms of excited-state dynamics and the interactions between local mode oscillators in the $M(CH_3)_4$ systems and in their deuterated isomers. In particular, we attempt to understand the differences in spectral structure by analyzing the efficiency of Fermi resonance coupling on the basis of energy criteria. This will require a knowledge of the nature and frequency of the normal vibrational modes in the three neopentane isomers and in TMS. Thus we obtain the frequencies of these modes through ab initio calculations. The methyl CH

10.1021/jp0209493 CCC: $22.00 © 2002 American Chemical Society
Published on Web 08/14/2002

bond length depends on the torsional angle, and this dependence implies a coupling of methyl librational or torsional modes with (1) CH stretching modes and (2) CH bending modes, both of which are implicated in Fermi resonance. We will examine these dependences and their implications for the deactivation of highly excited local mode states.

Given the high amplitude of vibration associated with excitation of up to eight CH stretching vibrational quanta, the possibility exists for intramolecular steric interactions in highly excited vibrational states. We identify these interactions as through space coupling in the sense that they promote vibrational deactivation both through effects on vibrational frequencies and through facilitation of torsion−stretch coupling. We will compare the probability of this interaction in neopentane and TMS and attempt to find spectral manifestations of through space coupling.

Experimental Section

Sample Preparation. Neopentane-d_0 (Matheson Gas Products, 99.87%), -d_6 (Fischer, 99.9+ at. %), and -d_9 (Fischer, 99.9+ at. %) were used without further purification. A gas chromatograph/mass spectrometer analysis revealed that the neopentane-d_0 sample contained no significant levels of impurities.

NMR grade TMS (Aldrich, 99.9+%) was obtained as a liquid and was degassed by repeated freeze−pump−thaw cycles. TMS was dried by passing it through molecular sieves prior to its introduction into a spectrometric gas cell.

Intracavity Laser Photoacoustic Spectroscopy. Our ICLPAS setup has been described elsewhere,[17,22−24] and only an abbreviated summary is given here. A 20 W Coherent Innova 200 argon ion laser is used to pump a Coherent 599 tunable dye laser or a broadband Coherent 890 Ti:sapphire (Ti:sapph) laser. In this work we use the short-wave and midwave optics in the Ti:sapph laser and the laser dyes DCM, Coumarin 6, and Coumarin 102. This combination enables us to scan a region from 9300 to 23 900 cm^{-1} ($\Delta v_{CH} = 4-9$). Tuning is accomplished via birefringent filters with resolutions of approximately 0.4 cm^{-1}, and spectra are referenced to known water lines, which results in an estimated error in peak position of 2 cm^{-1}.

The gas line and PA cell are evacuated to a pressure of 10^{-3} to 10^{-4} Torr for at least 4 h prior to sample introduction to ensure dryness.

Theory and Calculations

Local Modes of Vibration and the HCAO Model. The XH stretching overtone spectra can be interpreted within the local mode model of molecular vibration.[2,3] Within this model the XH stretching potential is often described as a Morse potential[9,25]

$$V(q) = D_e(1 - e^{-aq})^2 \tag{1}$$

where q is the displacement from the equilibrium XH bond length, D_e is the depth of the potential well

$$D_e = \frac{\tilde{\omega}^2}{4\tilde{\omega}x} \tag{2}$$

$\tilde{\omega}$ and $\tilde{\omega}x$ are the pure local mode frequency and anharmonicity (vide infra), respectively. The Morse scaling factor a is given by

$$a = \frac{\tilde{\omega}}{\hbar}\sqrt{\frac{\mu}{2D_e}} \tag{3}$$

where μ is the reduced mass of the XH oscillator. The energy eigenvalues of a Morse oscillator are given by[9,26]

$$\tilde{E}_v = \tilde{\omega}\left(v + \frac{1}{2}\right) - \tilde{\omega}x\left(v + \frac{1}{2}\right)^2 \tag{4}$$

Equation 4 can be rearranged to give the frequency $\tilde{\nu}_{v\leftarrow 0}$ of an overtone transition from the ground state to state v[9]

$$\tilde{\nu}_{v\leftarrow 0} = v\tilde{\omega} - (v^2 + v)\tilde{\omega}x \tag{5}$$

The values of the Morse parameters $\tilde{\omega}$ and $\tilde{\omega}x$ are obtained from a quadratic fit of $\tilde{\nu}_{v\leftarrow 0}$ vs v to (5). The eigenstates are obtained within the HCAO model[5,14−16] in terms of Morse oscillator wave functions[9] with the assumption of harmonic coupling between the CH oscillators.

Vibrational Overtone Lifetimes and Frequencies. The lifetimes τ of the pure local mode states of the neopentanes and TMS are calculated on the basis of their fwhm values using the equation[27]

$$\tau = (2\pi c\Gamma)^{-1} \tag{6}$$

where Γ is the fwhm of the transition in question and c is the speed of light. Thus we assume that the constituent Lorentzians that comprise a given band are homogeneously broadened.

Mean Oscillator Displacements and Morse Turning Points. The equilibrium XH oscillator bond length is denoted r_e. The mean displacement of an oscillator from r_e is the expectation value $\langle q\rangle$, and the standard deviation in $\langle q\rangle$, denoted $\sigma\langle q\rangle$, is given by

$$\sigma\langle q\rangle = \sqrt{\langle q^2\rangle - \langle q\rangle^2} \tag{7}$$

The classical outer or inner turning points of a Morse oscillator at a given vibrational excitation v can be obtained by equating (1) with (4) and solving for q. In practice, it is more convenient to solve iteratively for q at the classical outer or inner turning points than it is to obtain analytical solutions.

Coupling between Stretching and Torsional Motions. CH stretching modes couple to torsional modes through the dependence of $\tilde{\omega}$ and $\tilde{\omega}x$ on the dihedral (torsional) angle ϕ.[28−32] In the $M(CH_3)_4$ homologues this dependence can be approximated as a cosine squared function

$$\tilde{\omega}(\phi) = \tilde{\omega} + \delta_{\tilde{\omega}} \cos^2\left(\frac{3\phi}{2}\right) \tag{8}$$

where $\delta_{\tilde{\omega}} = \tilde{\omega}(0°) - \tilde{\omega}(60°)$ in which $\tilde{\omega}(60°)$ and $\tilde{\omega}(0°)$ are the local mode frequencies in the staggered and eclipsed conformers, respectively. The values of $\tilde{\omega}(60°)$ and $\tilde{\omega}(0°)$ are calculated using the method of Low and Kjaergaard[33] where, in our case, the ab initio value of $\tilde{\omega}(60°)$ is scaled to be identical to the experimentally obtained value of $\tilde{\omega}$. This scaling factor is then applied to the ab initio value of $\tilde{\omega}(0°)$.

Similarly, the ϕ dependence of $\tilde{\omega}x$ can be expressed as

$$\tilde{\omega}x(\phi) = \tilde{\omega}x + \delta_{\tilde{\omega}x} \cos^2\left(\frac{3\phi}{2}\right) \tag{9}$$

where $\delta_{\tilde{\omega}x} = \tilde{\omega}x(0°) - \tilde{\omega}x(60°)$ in which $\tilde{\omega}x(60°)$ and $\tilde{\omega}x(0°)$

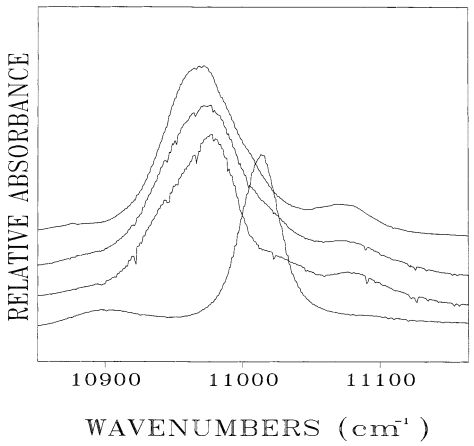

Figure 1. $\Delta v_{CH} = 4$ regions of the room-temperature ICL-PAS (Ti: sapph (mw)) spectra of neopentane-d_0, -d_6, and -d_9 and TMS at pressures ranging from 11.0 to 11.8 Torr (see Tables 1 and 2 and ref 17).

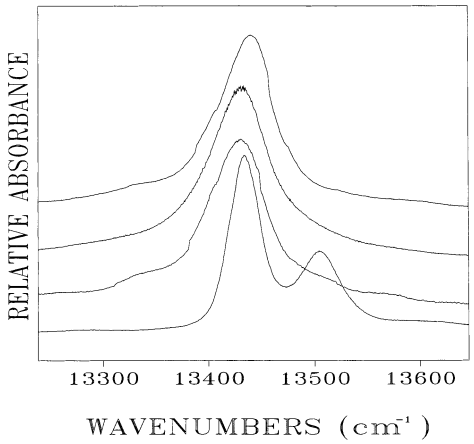

Figure 2. $\Delta v_{CH} = 5$ regions of the room-temperature ICL-PAS (Ti: sapph (sw)) spectra of neopentane-d_0, -d_6, and -d_9 and TMS at pressures ranging from 10.0 to 15.6 Torr (see Tables 1 and 2 and ref 17).

are the local mode anharmonicities in the staggered and eclipsed conformers. In a manner analogous to that in (8) the ab initio value of $\tilde{\omega}x(60°)$ is scaled to be identical to the experimental value of $\tilde{\omega}x$ and this scaling factor is subsequently applied to the ab initio value of $\tilde{\omega}x(0°)$[33].

Calculational Details. All ab initio geometry optimizations and frequency calculations are carried out with Gaussian 98 revision A.5[34] on an SGI Octane with a MIPS R10000 processor. Vibrational frequency calculations for deuterated species are requested in the route via Freq=ReadIsotopes. These vibrational analyses are carried out at reference geometries optimized at the same level of theory and basis set. Calculations use all Gaussian 98 defaults (unless noted otherwise) except that the Gaussian 98 overlay option IOP(3/32=2) is used with all calculations to prevent the reduction of expansion sets. In some instances subsequent refinements of calculated vibrational frequencies were carried out by reoptimizing the reference geometry at Opt=Tight and recalculating the vibrational frequencies specifying Int=UltraFine.[35]

Results and Discussion

Spectral Structure. The $\Delta v_{CH} = 4-8$ overtone spectra of neopentane-d_0, -d_6, and -d_9 and TMS are shown in Figures 1−5. The overtone profiles of the neopentanes are similar (but not identical) and, as noted previously,[17,20,21] much broader than the corresponding profiles for TMS. All spectra are deconvoluted

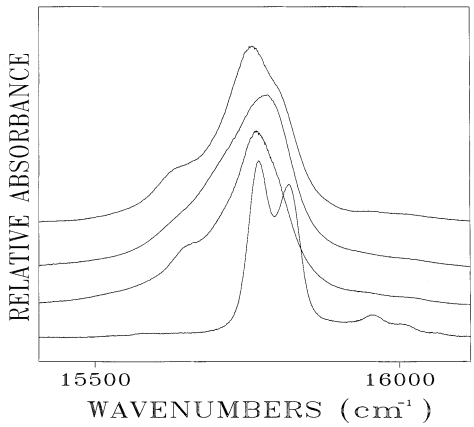

Figure 3. $\Delta v_{CH} = 6$ regions of the room-temperature ICL-PAS (DCM) spectra of neopentane-d_0, -d_6, and -d_9 and TMS at pressures ranging from 70.2 to 200.0 Torr (see Tables 1 and 2 and ref 17).

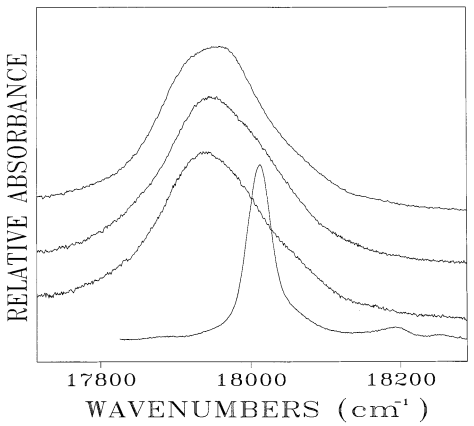

Figure 4. $\Delta v_{CH} = 7$ regions of the room-temperature ICL-PAS (Coumarin 6) spectra of neopentane-d_0, -d_6, and -d_9 and TMS at pressures ranging from 161.8 to 400.0 Torr (see Tables 1 and 2 and ref 17).

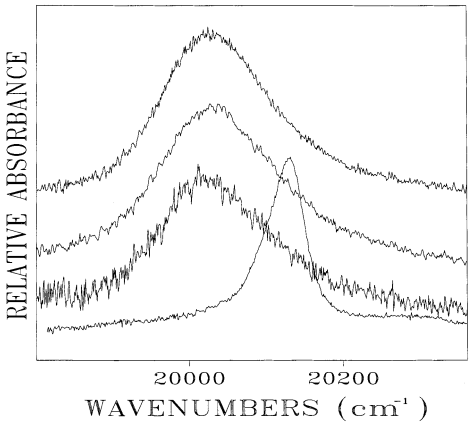

Figure 5. $\Delta v_{CH} = 8$ regions of the room-temperature ICL-PAS (Coumarin 102) spectra of neopentane-d_0, -d_6, and -d_9 and TMS at pressures of ≈ 450 Torr. The spectra are the sum of two scans.

in SpectraCalc[36] with the least number of constituent Lorentzian peaks needed to reproduce the experimental spectrum. The energies and fwhm values of the pure local mode transitions of neopentane-d_6 and -d_9 are obtained via deconvolution and are given in Tables 1 and 2. All spectral profiles required at least two Lorentzian peaks for deconvolution except TMS at $\Delta v_{CH} = 8$ where a single Lorentzian sufficed. The dominant peak is chosen to represent the pure local mode transition. In some cases component peaks have comparable intensities and the pure local

TABLE 1: Pure Local Mode Transition Peak Properties of Gaseous Neopentane-d_6

Δv_{CH}	spectrometer/ laser	gas pressure (Torr)	energy (cm^{-1})	fwhm[a] (cm^{-1})
3	Cary 5e[b]	215 ± 2	8409	54
4	Ti:sapph (mw)	11.4 ± 0.3	10976	68
5	Ti:sapph (sw)	15.0 ± 0.1	13429	73
6	DCM dye	200.0 ± 0.5	15722	164
7	Coumarin 6 dye	201.2 ± 0.4	17941	150
8[c]	Coumarin 102 dye	≈450	20038	183

[a] The full width at half-maximum of the dominant peak from the deconvolution. [b] See ref 17 for experimental conditions. [c] The spectrum is obtained by co-adding two spectra.

TABLE 2: Pure Local Mode Transition Peak Properties of Gaseous Neopentane-d_9

Δv_{CH}	spectrometer/ laser	gas pressure (Torr)	energy (cm^{-1})	fwhm[a] (cm^{-1})
3	Cary 5e[b]	48 ± 3	8407	41
4	Ti:sapph (mw)	11.4 ± 0.3	10979	44
5	Ti:sapph (sw)	15 ± 0.2	13428	65
6	DCM dye	200 ± 0.5	15770	100
7	Coumarin 6 dye	400 ± 0.5	17948	174
8[c]	Coumarin 102 dye	≈450	20033	179

[a] The full width at half-maximum of the dominant peak from the deconvolution. [b] See ref 17 for experimental conditions. [c] The spectrum is obtained by co-adding two spectra.

TABLE 3: Lifetimes of the CH Stretching Overtone States of Neopentane-d_0, -d_6, and -d_9 and TMS Excited by v Vibrational Quanta

	lifetime (fs)			
v	neopentane-d_0[a]	neopentane-d_6[b]	neopentane-d_9[c]	TMS[a]
3	110	99	130	130
4	92	78	120	170
5	92	73	81	120
6	53	32	53	120
7	36	35	31	150
8	31	29	30	150
9	44			

[a] Calculated with eq 6 and data from ref 17. [b] Calculated with eq 6 and data from Table 1. [c] Calculated with eq 6 and data from Table 2.

mode transition is identified as the one that gives the best fit to eq 5.

Previously, the asymmetry in the TMS $\Delta v_{CH} = 4-6$ spectra has been ascribed to a Fermi resonance where a pure local mode $|v, 0, 0\rangle$ state mixes with a local mode-normal mode combination state with a local mode component $|v - 1, 0, 0\rangle$ and a normal mode component $|2v_b\rangle$ (where $|v_b\rangle$ is typically a bending mode).[17,20] Fermi resonances can provide rapid pathways for energy flow out of CH oscillators via IVR.[37] The rate of flow of energy out of these local mode-normal mode states (and therefore the spectral fwhm) is also governed by subsequent coupling into other dark bath states. The Fermi resonance in TMS is tuned and detuned[38] in moving from $\Delta v_{CH} = 4$ to $\Delta v_{CH} = 6$. Nevertheless, the excited state lifetimes of TMS (from (6) and the data of ref 17) are found to be more or less invariant (Table 3), ranging from 120 to 170 fs. Such lifetimes are on the time scale of strong, preferentially coupled anharmonic vibrational modes.[39] Owing to their short lifetimes, the de-excitation of the local mode states by processes such as intermolecular collisions would not occur under our experimental conditions.

The excited-state lifetimes of the neopentanes are determined in a manner identical to that for TMS from published data[17] for neopentane-d_0 and from the data contained in Tables 1 and 2 for neopentane-d_6 and neopentane-d_9, respectively. The lifetimes of the CH stretching local mode states of the neopentanes are presented in Table 3 and range from approximately 30 to 100 fs. As in the case of TMS, the de-excitation of the local mode states of the neopentanes by processes such as intermolecular collisions is not plausible. The decrease in lifetimes of the neopentanes (as compared to TMS and other $M(CH_3)_4$ homologues[20]) indicates an increased efficiency in the coupling of local mode states into dark states. Asymmetries in the spectral profiles of the neopentanes are the frequency domain manifestations of such couplings.

TABLE 4: Ideal Frequencies for (2:1), (3:1), and (4:1) Vibrational Resonances[a] between the $|v, 0, 0\rangle$ and $|v - 1, 0, 0\rangle|nv_b\rangle$ States of Neopentane-d_0 and TMS

	neopentane-d_0			TMS		
Δv_{CH}	(2:1)	(3:1)	(4:1)	(2:1)	(3:1)	(4:1)
0	1525	1016	762	1522	1014	761
1	1464	976	732	1463	975	731
2	1404	936	702	1404	936	702
3	1343	895	672	1345	897	673
4	1282	855	641	1287	858	643
5	1222	815	611	1228	819	614
6	1161	774	581	1169	780	585
7	1101	734	550	1111	740	555
8	1040	694	520	1052	701	526
9	980	653	490	993	662	497

[a] The energies of the states are calculated using eqs 4 and 10. The local mode parameters for neopentane-d_0 and TMS are from ref 17 (see also Table 11).

Coupling Mechanisms. Fermi resonance couples an initially prepared excited pure local mode state $|v, 0, 0\rangle$ with a near-resonant state $|v - 1, 0, 0\rangle|nv_b\rangle$ and these latter states act as "doorway states" into the vibrational bath.[18,38,40] In $M(CH_3)_4$ molecules, Fermi resonance and subsequent coupling into the bath are influenced by through space coupling. This through space coupling can modify the vibrational potential energy surface for normal modes and shift the vibrational frequencies of $|v_b\rangle$ states into a range where efficient Fermi resonances can occur. It can also mix torsional and vibrational states, which serves to increase the density of final states and thus to accelerate IVR.[41] We will first consider Fermi resonance in the absence of through space coupling and begin by calculating the normal-mode frequencies.

Ab Initio Calculated Normal-Mode Frequencies. It is useful to introduce the concept of "ideal" frequencies for (n:1) resonances, $\tilde{\nu}_{|v_{b,ideal}\rangle}$, between the states $|v, 0, 0\rangle$ and $|v - 1, 0, 0\rangle|nv_b\rangle$

$$\tilde{\nu}_{|v_{b,ideal}\rangle} = \frac{E_{|v,0,0\rangle} - E_{|v-1,0,0\rangle}}{n} \tag{10}$$

The closer a normal-mode frequency of vibration with the correct symmetry is to $\tilde{\nu}_{|v_{b,ideal}\rangle}$, the more efficient is the coupling of states $|v, 0, 0\rangle$ and $|v - 1, 0, 0\rangle|nv_b\rangle$ (provided that the coupling matrix element is sufficiently large). The values of $\tilde{\nu}_{|v_{b,ideal}\rangle}$ for $n = 2-4$ in neopentane-d_0 and TMS are given in Table 4 (values of $\tilde{\nu}_{|v_{b,ideal}\rangle}$ for neopentane-d_6 and -d_9 are identical to those of neopentane-d_0 within experimental error). The range of $\tilde{\nu}_{|v_{b,ideal}\rangle}$ frequencies relevant to coupling in the (2:1) through (4:1) mechanisms in both the neopentanes and TMS is approximately 500−1500 cm^{-1}.

The normal mode vibrational frequencies of neopentane-d_0 and TMS are calculated at B3LYP, B3PW91, and MPW1PW91 levels of theory with numerous basis sets. Following the example of Rauhut and Pulay,[42] as well as Baker, Jarzecki, and Pulay,[43]

TABLE 5: Frequencies of the Normal Modes of Vibration of Neopentane-d_0

		frequency (cm^{-1})			
mode	no.	present work[a]	calculated[b]	infrared[c]	Raman[b]
A_2	1	202	239		
T_1	2	279	308		
E	3	331	335		**334**
T_2	4	418	415	418	**416**
A_1	5	732	733		**733**
T_2	6	926	921	925	**931**
T_1	7	945	953		
E	8	1070	1075		
T_2	9	1262	1249	1256	**1256**
T_2	10	1376	1365	**1372**	
A_1	11	1413	1400		
T_1	12	1446	1444		
E	13	1454	1451		**1467**
T_2	14	1483	1477	**1475**	
T_2	15	2891	2863	2876	**2874**
A_1	16	2901	2909		**2923**
T_1	17	2960	2954		
E	18	2960	2955		**2963**
T_2	19	2967	2959	**2959**	

[a] Calculations are performed at B3LYP/cc-pVDZ. Geometry optimized at Opt=Tight and frequency calculated requesting Int=UltraFine. Training set frequencies are in bold. A scaling factor of 0.997 is employed in the fingerprint region (500−2500 cm^{-1}), whereas scaling factors of 1.013 and 0.959 are employed in the pre- and postfingerprint regions. [b] From ref 50. [c] From ref 68.

TABLE 6: Frequencies of the Normal Modes of Vibration of TMS

		frequency (cm^{-1})			
mode	no.	present work[a]	calculated[b]	infrared[c]	Raman[d]
A_2	1	149	153		
T_1	2	173	157		
E	3	191	180		**190.5**
T_2	4	239	223		**239**
A_1	5	570	573		**593**
T_1	6	683	690		
T_2	7	684	683	**696**	698
E	8	825	827	**871**	870
T_2	9	873	879		
T_2	10	1264	1264	**1253**	1257
A_1	11	1277	1270		**1271**
T_1	12	1427	1417		
E	13	1431	1433		**1421**
T_2	14	1446	1419	**1430**	
T_2	15	2894	2891	**2900**	
A_1	16	2897	2888		**2913**
E	17	2970	2960		**2964**
T_1	18	2971	2964		
T_2	19	2973	2961	**2957**	

[a] Calculations are performed at B3LYP/cc-pVDZ. Geometry optimized at Opt=Tight and frequency calculated requesting Int=UltraFine. Training set frequencies are in bold. A scaling factor of 0.999 is employed in the fingerprint region (500−2500 cm^{-1}), whereas scaling factors of 1.032 and 0.958 are employed in the pre- and postfingerprint regions. [b] From ref 50. [c] From ref 68.

we divide the vibrational spectra of molecules into three regions, namely, the fingerprint region (500−2500 cm^{-1}), as well as prefingerprint (below 500 cm^{-1}) and postfingerprint (above 2500 cm^{-1}) regions. One empirical scaling factor (vide infra) is derived for each of these regions, at each level of theory and basis set, to correct for anharmonic effects and the deficiencies of the quantum chemical method.[44] The training sets that we use to obtain scaling factors for neopentane-d_0 and TMS are indicated in Tables 5 and 6. The RMS deviations of scaled

TABLE 7: Root Mean Square Deviations (cm^{-1}) from Training Seta of the Calculated Fundamentals for Neopentane from Various Scaled Correlation Functions and Basis Sets

	frequency range (cm^{-1})		
theory/basis set	0−500	500−2500	>2500
B3LYP/6-31G(d)	2.4	17.6	14.0
B3LYP/6-31G(d,p)	2.3	14.7	14.3
B3LYP/6-311++G(d,p)	1.8	13.2	14.1
B3LYP/6-311++G(2d,2p)	1.9	15.2	14.6
B3LYP/cc-pVDZ	2.7	7.2	14.4
B3LYP/cc-pVDZ $_{uf}$[b]	2.5	7.2	13.8
B3LYP/aug-cc-pVDZ	3.1	7.6	13.9
B3LYP/cc-pVTZ	2.3	13.3	14.4
B3PW91/6-31G(d)	1.4	12.0	15.3
B3PW91/6-31G(d,p)	1.3	9.5	16.2
B3PW91/6-311++G(d,p)	0.6	8.2	15.0
B3PW91/6-311++G(2d,2p)	0.7	9.1	14.9
B3PW91/cc-pVDZ	1.7	9.2	17.0
MPW1PW91/6-31G(d)	1.2	10.4	15.6
MPW1PW91/6-31G(d,p)	1.1	8.4	16.6
MPW1PW91/6-311++G(d,p)	0.3	7.4	15.2
MPW1PW91/6-311++G(2d,2p)	0.4	7.9	15.0
MPW1PW91/cc-pVDZ	1.4	15.5	20.0
literature[c]	1.0	8.7	9.3

[a] Training set frequencies are given in Table 5 in bold. [b] Geometry optimized at Opt=Tight, frequencies calculated at Int=UltraFine. [c] From ref 50.

TABLE 8: Root Mean Square Deviations (cm^{-1}) from Training Set[a] of the Calculated Fundamentals for TMS from Various Scaled Correlation Functions and Basis Sets

	frequency range (cm^{-1})		
theory/basis set	0−500	500−2500	>2500
B3LYP/6-31G(d)	1.8	30.8	8.6
B3LYP/6-31G(d,p)	1.8	26.8	10.8
B3LYP/6-311++G(d,p)	1.8	24.0	7.5
B3LYP/6-311++G(2d,2p)	1.5	25.5	6.3
B3LYP/cc-pVDZ	2.4	20.9	11.9
B3LYP/cc-pVDZ $_{uf}$[b]	0.2	21.7	11.8
B3PW91/6-31G(d)	2.2	27.7	13.1
B3PW91/6-31G(d,p)	2.3	24.1	15.5
B3PW91/6-311++G(d,p)	2.3	22.4	12.3
B3PW91/6-311++G(2d,2p)	1.8	24.1	10.8
MPW1PW91/6-31G(d)	2.1	27.7	13.6
MPW1PW91/6-31G(d,p)	2.1	24.1	16.1
MPW1PW91/6-311++G(d,p)	2.2	22.7	12.8
literature[c]	13.5	69.1	12.7

[a] Training set frequencies are given in Table 6 in bold. [b] Geometry optimized at Opt=Tight, frequencies calculated at Int=UltraFine. [c] From ref 50.

frequencies from the training set for neopentane-d_0 and TMS are indicated in Tables 7 and 8.

The smallest RMS deviations from training set frequencies in the frequency range of interest (i.e., fingerprint region) are obtained for both neopentane-d_0 and TMS using Becke's three-parameter hybrid method[45,46] with the Lee−Yang−Parr[47,48] correlation functional, B3LYP, and Dunning's[49] cc-pVDZ correlation consistent basis set. Vibrational frequencies are further refined at B3LYP/cc-pVDZ by optimizing the reference geometry at Opt=Tight and recalculating the frequencies with the (UltraFine) pruned (99, 590) grid. These refined frequencies are presented along with the calculated frequencies of Zarkova et al.[50] in Tables 5 and 6. Our RMS deviations are comparable to those of ref 50 in the 500−2500 cm^{-1} range for neopentane-d_0 and significantly smaller for TMS.

To our knowledge, the normal mode vibrational frequencies of neopentane-d_6 and -d_9 have not been reported previously. In

TABLE 9: Calculated Frequencies (B3LYP/cc-pVDZ)[a] of the Normal Modes of Vibration of Neopentane-d_6[b]

mode	no.	frequency[c] (cm^{-1})	mode	no.	frequency[c] (cm^{-1})
A_2	1	158	A_1	24	1090
B_1	2	201	B_1	25	1225
A_2	3	254	A_1	26	1249
B_2	4	278	B_2	27	1260
A_1	5	296	B_1	28	1377
A_2	6	304	A_1	29	1395
B_1	7	371	A_2	30	1450
B_2	8	390	B_1	31	1455
A_1	9	390	A_1	32	1469
A_1	10	682	B_2	33	1473
B_2	11	732	B_2	34	2158
A_2	12	767	A_1	35	2163
B_1	13	781	A_2	36	2279
A_1	14	806	B_2	37	2279
B_2	15	882	A_1	38	2281
B_1	16	937	B_1	39	2282
A_1	17	987	B_1	40	2891
A_2	18	1022	A_1	41	2896
B_2	19	1047	A_2	42	2960
A_2	20	1047	B_1	43	2960
A_1	21	1054	A_1	44	2963
B_1	22	1055	B_2	45	2965
B_2	23	1071			

[a] Geometry optimized at Opt=Tight and frequency calculated requesting Int=UltraFine. [b] The point group symmetry of neopentane-d_6 is C_{2v}. The molecule is oriented with the C_2 axis along the *z*-axis and the CH_3 groups in the *xz*-plane. [c] A scaling factor of 0.997 is employed in the fingerprint region (500−2500 cm^{-1}), whereas scaling factors of 1.013 and 0.959 are employed in the pre- and postfingerprint regions.

TABLE 10: Calculated Frequencies (B3LYP/cc-pVDZ)[a] of the Normal Modes of Vibration of Neopentane-d_9[b]

mode	no.	frequency[c] (cm^{-1})	mode	no.	frequency[c] (cm^{-1})
A_2	1	149	A_1	16	1058
E	2	200	E	17	1066
A_2	3	265	A_1	18	1093
E	4	287	A_1	19	1217
A_1	5	354	E	20	1245
E	6	371	A_1	21	1386
A_1	7	662	E	22	1462
A_2	8	717	E	23	2158
E	9	741	A_1	24	2166
A_1	10	795	A_2	25	2278
E	11	801	E	26	2279
E	12	953	E	27	2281
A_2	13	1043	A_1	28	2283
E	14	1046	A_1	29	2893
E	15	1054	E	30	2962

[a] Geometry optimized at Opt=Tight and frequency calculated requesting Int=UltraFine. [b] The point group symmetry of neopentane-d_9 is C_{3v}. [c] A scaling factor of 0.997 is employed in the fingerprint region (500−2500 cm^{-1}), whereas scaling factors of 1.013 and 0.959 are employed in the pre- and postfingerprint regions.

Tables 9 and 10 we present the scaled (vide infra) ab initio frequencies of these molecules from B3LYP/cc-pVDZ calculations performed with the (UltraFine) pruned (99, 590) grid from a reference geometry optimized at Opt=Tight.

The scaling of neopentane-d_6 and -d_9 vibrational frequencies is carried out with the same empirical scaling factors that are used for neopentane-d_0. Simple empirical scaling factors were used in favor of more elaborate frequency scaling approaches such as the separate treatment of chemically distinct stretching and bending modes[44] or the direct scaling of primitive valence force constants[43] because of their ease of implementation. The use of a single scaling factor for CH, CD, and CC bonds in a given spectral region is not unreasonable as Rauhut and Pulay[42] found that CH and CX (where X is any heavy atom) stretch scaling factors at B3LYP/6-31G(d) are nearly identical.

Magdó et al.[44] determined that the scaled force constant of a XD bond F_{XD} is related to the scaled force constant of a XH bond F_{XH} through the Morse oscillator model anharmonic correction factor σ_{XD}

$$F_{XD} = \sigma_{XD} F_{XH} \tag{11}$$

where σ_{XD} can be expressed as

$$\sigma_{XD} = \left(\frac{1 - 2\tilde{\omega}x/\tilde{\omega}\sqrt{\mu_{XH}/\mu_{XD}}}{1 - 2\tilde{\omega}x/\tilde{\omega}} \right)^2 \tag{12}$$

where μ_{XH} and μ_{XD} are respectively the reduced masses of XH and XD oscillators. Kjaergaard, Turnbull, and Henry have published[51] CH and CD local mode frequencies and anharmonicities for 1,3-butadiene and 1,3-butadiene-d_6. From their values of $\tilde{\omega}$ and $\tilde{\omega}x$, the anharmonic correction factors σ_{XD} that relate the three nonequivalent CD bonds in 1,3-butadiene-d_6 to the three nonequivalent CH bonds in 1,3-butadiene are calculated from (12). The values of the anharmonic force constant correction factor σ_{XD} range from 1.013 to 1.015. The fact that σ_{XD} is nearly unity indicates that to a first approximation using the same vibrational frequency scaling factors for CH and CD bonds in hydrocarbons is not unreasonable.

Experimental Evidence for Fermi Resonance. Calculated normal mode transition frequencies can be used to predict the presence of Fermi resonances between the states $|v, 0, 0\rangle$ and $|v - 1, 0, 0\rangle|nv_b\rangle$. In TMS we note that the calculated normal mode transition frequencies of vibrational modes 10 and 11 (Table 6) are very close in energy to the "ideal" (2:1) resonance frequencies for the pure local mode states prepared by the transitions $\Delta v_{CH} = 4$ and 5. Fermi resonances in TMS are observed as two distinct peaks in Figures 1 and 2. Similarly, we note that neopentane-d_0 vibrational modes 6−8 (Table 5) are close to the (2:1) $\tilde{\nu}_{|v_{b,ideal}\rangle}$ values for the pure local mode states prepared by the transitions $\Delta v_{CH} = 7-9$. Modes 16−24 in neopentane-d_6 (Table 9) and modes 12−18 in neopentane-d_9 (Table 10) are also close to (2:1) $\tilde{\nu}_{|v_{b,ideal}\rangle}$ values for the pure local mode states prepared by the transitions $\Delta v_{CH} = 7-9$. States prepared by transitions $\Delta v_{CH} = 4$ and 5 have (2:1) $\tilde{\nu}_{|v_{b,ideal}\rangle}$ values close to the frequencies of vibrational mode 9 in neopentane-d_0, modes 25−27 for neopentane-d_6, and modes 19 and 20 for neopentane-d_9. Unlike TMS the overtone transitions of the neopentanes do not resolve neatly into two distinct peaks characteristic of a specific Fermi resonance. The local modes states $|v, 0, 0\rangle$ in the neopentanes are likely to be in resonance with more than one $|v - 1, 0, 0\rangle|nv_b\rangle$ local mode−normal mode combination state. In addition, other interactions (vide infra) could affect coupling. The asymmetries and structure of the transitions in the neopentanes in Figures 1−5 indicate that strong couplings with states $|v, 0, 0\rangle$ are occurring.

The frequency data indicate that Fermi resonance could be expected to be more efficient in the neopentanes than in TMS because of a greater number of matching states. However, this argument by itself does not appear to account for the dramatic spectral differences. For example, a strong Fermi resonance in TMS is observed at $\Delta v_{CH} = 6$ (Figure 3), however, the calculated normal modes of vibration in TMS do not correspond well with (2:1) $\tilde{\nu}_{|v_{b,ideal}\rangle}$ at $\Delta v_{CH} = 6$, even if one allows several times the estimated 22 cm^{-1} RMS error in frequency (Table 8). Similarly, strong resonances are evident at $\Delta v_{CH} = 6$ (Figure

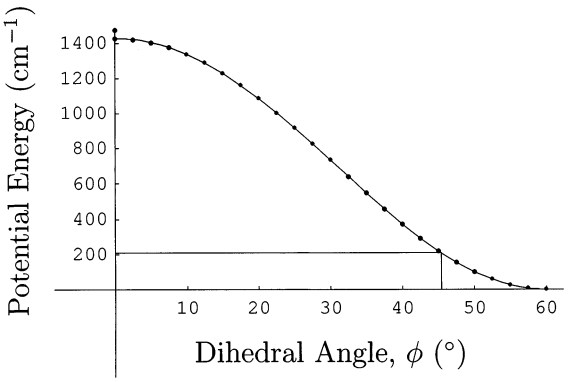

Figure 6. Ab initio potential energy barrier to internal methyl rotation in neopentane-d_0 calculated at HF/6-311+G(d,p).

3) in the neopentanes, yet the agreement of (2:1) $\tilde{\nu}_{|\upsilon_{b,ideal}\rangle}$ at $\Delta\upsilon_{CH} = 6$ with the frequencies of the available states $|\upsilon_b\rangle$ is poor. Thus, although vibrational analysis of these molecules in their stationary reference geometries can predict the presence of some Fermi resonances, there appears to be a need to include dynamic effects when normal mode vibrational frequencies of highly vibrationally excited molecules are calculated.

Methyl Librational Effects. Librational motion occurs when a hindered rotor cannot surmount the barrier to internal rotation. Barriers to internal methyl rotation in neopentane-d_0 are calculated (neglecting zero point energies) with the cc-pVDZ basis set using B3LYP, B3PW91, and MPW1PW91 levels of theory. These barriers are respectively 1330, 1350, and 1370 cm^{-1}. Similar calculations using HF theory and the basis sets 6-311+G(d,p), 6-311++G(d,p), and 6-311++G(2d,2p) all give barrier heights of 1430 cm^{-1}. Calculated barriers to internal methyl rotation where zero point energies are neglected are found to be 520, 530, and 540 cm^{-1} in TMS using the cc-pVDZ basis and (respectively) B3LYP, B3PW91, and MPW1PW91 levels of theory. Similar calculations with HF theory and the basis sets 6-311+G(d,p), 6-311++G(d,p), and 6-311++G(2d,-2p) give respective barrier heights of 570, 570, and 580 cm^{-1}. Neopentane and TMS therefore undergo internal methyl libration, as opposed to internal rotation, at room temperature.

Librational motion can promote the mixing of torsional and stretching motions. From the ab initio HF/6-311+G(d,p) potential energy barrier to internal methyl rotation in neopentane-d_0 (Figure 6) we note that there is sufficient energy at kT (207 cm^{-1}) for the highly hindered methyl rotor in this molecule to sample nearly 15° to either side of the lowest energy conformer ($\phi = 60°$). Palmö, Mirkin, and Krimm have found that CC force constants in neopentane depend on the methyl torsional angle,[52] and that CH force constants are coupled to CC force constants. The coupling between CH vibrational frequencies and methyl torsional angle can also be seen in the dependence of local mode parameters $\tilde{\omega}$ and $\tilde{\omega}x$ on ϕ given by eqs 8 and 9 and the parameters $\delta_{\tilde{\omega}}$ and $\delta_{\tilde{\omega}x}$ (Table 11).[28−32] The change in local mode transition frequencies resulting from varying ϕ from 60° to 45° are calculated using the data in Table 11 and eqs 5, 8, and 9. As the torsional angle changes from $\phi = 60°$ to 45°, the local mode transition frequency increases. In neopentane-d_0 this increase ranges from 1.2 cm^{-1} at $\Delta\upsilon_{CH} = 1$ to 7.7 cm^{-1} at $\Delta\upsilon_{CH} = 9$, whereas for TMS it ranges from 0.7 cm^{-1} at $\Delta\upsilon_{CH} = 1$ to 5.6 cm^{-1} at $\Delta\upsilon_{CH} = 9$. Note that the values of $\delta_{\tilde{\omega}}$ and $\delta_{\tilde{\omega}x}$ are significantly smaller for TMS. Thus, torsional−stretching mixing will be stronger in neopentane.

Methyl libration also affects lower frequency modes. In general, vibrational and torsional motions in a molecule are not separable, because motions along a vibrational coordinate distort the torsional potential and vice versa.[41] Thus de-excitation of vibrational modes on hindered rotors is expected to be very rapid as, classically, large energy flows occur when rotors cannot surmount the barrier to internal rotation. Changes in rotor momentum are large, resulting in periodic energy flows between individual oscillators and torsional modes, facilitating rapid IVR.[37] The barrier to internal methyl rotation is larger in neopentane than in TMS (vide supra). This larger barrier height causes both higher torsional energy levels and greater spacing between those levels. As a consequence changes in rotor momentum are larger in neopentane than in TMS for rotors at a given torsional energy level and for rotors undergoing transitions between torsional levels. Thus, we expect coupling between libration and other modes to be more efficient in neopentane than in TMS.

TABLE 11: Experimental and Theoretical Local Mode Parameters for Neopentane-d_0 and TMS

	parameter (cm^{-1})			
molecule	$\tilde{\omega}$	$\delta_{\tilde{\omega}}$	$\tilde{\omega}x$	$\delta_{\tilde{\omega}x}$
neopentane-d_0	3049 ± 2^a	$8.68^{b,c}$	60.5 ± 0.3^a	$0.285^{b,d}$
TMS	3043 ± 1^a	$4.87^{b,e}$	58.7 ± 0.2^a	$0.0606^{b,f}$

[a] From ref 17. [b] Calculated ab initio at HF/6-311+G(d,p) in a manner similar to that in ref 33 for CH bond lengths between $r_e - 0.20$ Å and $r_e + 0.20$ Å in steps of 0.05 Å from the staggered and eclipsed conformations. [c] Scaled by 0.9533. [d] Scaled by 0.8210. [e] Scaled by 0.9520. [f] Scaled by 0.7978.

Vibrational Analysis at Nonstationary Geometries. The frequency results of a vibrational analysis depend strongly upon the choice of a reference geometry. Vibrational energy levels depend mainly upon two contributions to the total potential energy $V(q,\phi)$ of a molecule, viz. nuclear−nuclear repulsion V_N and electronic energy E_e.[53] At large amplitudes of oscillator displacement (such as those accompanying vibrational overtone transitions) the higher order bond displacement terms q in a power expansion of $V(q,\phi)$ are expected to become increasingly important. High order bond stretching terms in $V(q,\phi)$ are very sensitive to core−core nuclear repulsions and thus to the reference geometries at which they are evaluated.[54]

We assume an adiabatic separation between large amplitude (overtone) stretching vibrations and lower amplitude harmonic vibrations,[28,54−56] including torsional modes. Thus low-frequency skeletal modes in TMS and the neopentanes should "see" an averaged local mode of vibration. The mean CH oscillator displacements in local mode states $|\upsilon, 0, 0\rangle$, denoted $\langle q\rangle$, and their associated standard deviations $\sigma\langle q\rangle$ (7) are calculated for neopentane-d_0 and TMS and are given in Table 12. The nonzero values of $\langle q\rangle$ reflect the nonsymmetric shape of the CH stretching potential, which is caused by its anharmonic nature. The high values of $\sigma\langle q\rangle$ reflect the result of the probabilistic interpretation of the wave function that the highest probability for the oscillator lies increasingly closer to the two extrema of motion (Table 12) with increasing vibrational excitation. Thus a CH oscillator in an excited local mode of vibration samples both repulsive inner ($\langle q\rangle - \sigma\langle q\rangle < 0$) and outer ($\langle q\rangle + \sigma\langle q\rangle > 0$) regions of $V(q,\phi)$ at $\Delta\upsilon_{CH} = 0-8$. However, the steepness of the CH stretching potential at the inner turning point and the relative flatness of the potential at the outer turning point cause the wave function to decay much more rapidly below the inner turning point than above the outer turning point. The nonsymmetric shape of the CH stretching potential leads to the consequence that the largest probability for a vibrationally excited oscillator lies at the outer turning point. These effects become more pronounced higher in the vibrational potential such that the sampling of the outer region of $V(q,\phi)$ increases rapidly

TABLE 12: Mean CH Oscillator Displacements $\langle q \rangle$, Their Standard Deviations $\Sigma\langle q \rangle$, and Morse Classical Turning Points[a] (pm) of the Overtone Vibrational Energy Levels of Neopentane-d_0 and TMS

	neopentane-d_0			TMS		
		turning point			turning point	
v	$\langle q \rangle \pm \sigma\langle q \rangle$	inner	outer	$\langle q \rangle \pm \sigma\langle q \rangle$	inner	outer
0	1.7 ± 7.8	−10	12	1.6 ± 7.8	−10	12
1	5.1 ± 14	−16	23	5.0 ± 14	−16	23
2	8.7 ± 18	−20	31	8.5 ± 18	−20	31
3	12 ± 21	−23	39	12 ± 21	−23	39
4	16 ± 25	−25	46	16 ± 25	−25	46
5	21 ± 28	−27	53	20 ± 28	−27	53
6	25 ± 30	−28	61	25 ± 30	−28	60
7	30 ± 33	−29	68	29 ± 33	−30	68
8	35 ± 36	−31	76	34 ± 36	−31	75
9	40 ± 39	−32	83	40 ± 38	−32	83

[a] Calculated with the local mode parameters form ref 17.

with increasing vibrational excitation. This modulation in nuclear displacement will lead to changes in V_N that will effect $V(q,\phi)$, and therefore the normal mode vibrational frequencies. A proper vibrational analysis of a molecule must therefore take into account the degree of molecular vibrational excitation. Moreover, most of the $\tilde{\nu}_{|v_{b,ideal}\rangle}$ frequencies (Table 4) are typical of low-frequency bend terms that, along with weak intermolecular interactions, are more strongly influenced by nonstationary reference geometries than are high-frequency stretching modes.[54] Quantitative calculations of vibrational frequencies in nonstationary reference geometries are, however, difficult.[53] In particular, the contamination of vibrational modes by rotational and translational modes can occur if nonzero forces exist.[35]

The data of Table 12 indicate that effects on lower frequency modes are expected to occur for higher overtone states because of changes in V_N caused by an increase in the average CH internuclear distance with increasing v. Such frequency changes will affect energy matching of states for Fermi resonance. The change in $\langle q \rangle$ is similar in neopentane and TMS. Resultant effects on Fermi resonance are difficult to predict. However, because of the higher degree of steric hindrance to large amplitude vibrational motion in neopentane than in TMS (vide infra), we expect the potential $V(q,\phi)$ to rise more sharply with increasing $\langle q \rangle$ for neopentane. Owing to this difference in $V(q,\phi)$ between neopentane and TMS, we expect nonstationary effects to be more pronounced in neopentane.

Through Space Coupling. Through space (or "collision-like") interactions have been postulated by Bellamy[57] as well as by Horák and Plíva.[58] Later work by Palmö et al.[52] showed that in branched chain hydrocarbons the CC stretching and bending force constants depend on the number of hydrogens attached to the carbon atoms, and a 9−6 potential for the nonbonded interactions between C and H atoms in neopentane was proposed. In aromatic systems it was found that such collision-like through space interactions between the methyl group and the aromatic ring in *p*-fluorotoluene lead to mixing between internal rotor levels and ring vibrations.[41] This concept was extended by suggesting that very rapid (tens of picoseconds) mixing occurs between internal rotor states and low-frequency ring modes, and a slower mixing occurs between rotor states and high-frequency ring modes.[59] The coupling between low-frequency aromatic ring modes and nearly free methyl internal rotation is thought to be crucial to the promotion of vibrational state mixing in that it allows states of different symmetries to mix to facilitate rapid IVR.[60,61] Whereas high barriers to internal methyl rotation, such as those in the neopentanes and TMS, will reduce the density of states with which coupling can occur, strong stretch−torsion interactions can lead to substantial mixing.

One indication of the strength of a through space interaction for an excited local mode of vibration is its deviation from Morse oscillator behavior. An intramolecular collision-like interaction between a vibrationally excited XH oscillator and some other part of the molecule will distort the XH vibrational potential away from the form given by (1). The Morse parameters $\tilde{\omega}$ and $\tilde{\omega}x$ are obtained from a fit of experimental data to (5). The variance s^2 from (5) given by $\sum^v(\tilde{\nu}_{v\leftarrow 0,\mathrm{calc}} - \tilde{\nu}_{v\leftarrow 0,\mathrm{exp}})^2/(N-2)$, where N is the number of data points, provides a statistical measure of the deviation from Birge−Sponer behavior. An analysis of the published vibrational overtone transition frequencies of *cis*- and *trans*-2-butene[62] shows that the estimated variances are influenced by through space interactions. In both *cis*- and *trans*-2-butene there are three unique types of CH oscillators. In the range $\Delta v_{CH} = 3-9$ the value of s^2 for the least sterically hindered CH oscillator in *cis*-2-butene is 0.08 cm^{-2} and that for the most sterically hindered CH oscillator is 9 cm^{-2}. In *trans*-2-butene, which is more sterically hindered than *cis*-2-butene, the least hindered CH oscillator has an s^2 of 0.1 cm^{-2} and the most sterically hindered CH oscillator has a variance of 10 cm^{-2}. As expected, variances indicate that through space interactions are stronger in the more sterically hindered molecules neopentane-d_0 and TMS.[17] In TMS the s^2 value calculated from data in the range $\Delta v_{CH} = 3-8$ is 39 cm^{-2} and the s^2 value for neopentane-d_0 calculated from data in the range $\Delta v_{CH} = 3-9$ is 103 cm^{-2}.

Through space interactions could occur in the neopentanes and TMS between the vibrationally excited hydrogen atoms on one methyl group and the proximal hydrogen (or deuterium) atoms on the remaining CH_3 or CD_3 groups. "Collisions" between these atoms are approximated as interactions between hard spheres whose volumes are determined from van der Waals parameters. To properly account for such through space interactions, one must take into account the geometry of the molecule and the van der Waals radii of the individual atoms. In particular, it is important to know $r_{HH,space}$, the separation between the nuclear centers of a hydrogen atom on one methyl group and the proximal hydrogen (or deuterium) atoms on the remaining CH_3 or CD_3 groups.

Values of $r_{HH,space}$ are obtained from both ab initio and experimentally determined geometries. Ab initio geometries are calculated for neopentane using B3LYP theory and the basis sets cc-pVNZ and aug-cc-pVNZ (where N = D or T). Geometries are also determined using the cc-pVDZ basis set with B3PW91 and MPW1PW91 levels of theory. Ab initio calculated values of $r_{HH,space}$ range from 255.8 pm at MPW-1PW91/cc-pVDZ to 257.2 pm at B3LYP/cc-pVDZ. Gas-phase electron diffraction experimental data lead to $r_{HH,space}$ values of 253.1 pm[63] and 259.0 pm.[64] The van der Waals radius for a hydrogen atom is 120 ± 5 pm.[65] In the absence of methyl torsion the separation between the volumes occupied by the hydrogen atoms on different methyl groups in the same molecule in the neopentanes ranges from 13 to 19 pm. The classical turning points of the CH oscillators in neopentane-d_0 and TMS are calculated iteratively from eqs 1 and 4 (Table 12), neglecting the penetration of the CH stretching wave function into the nonclassical region (vide supra). In neopentane-d_0 the classical outer turning points range from 12 pm beyond the equilibrium CH separation at $\Delta v_{CH} = 0$ to 83 pm beyond the equilibrium CH separation at $\Delta v_{CH} = 9$. Significant increases in the fwhm values of the (deconvoluted) local mode overtone transitions

of neopentane-d_0 have been observed in going from $\Delta v_{CH} = 5$ to $\Delta v_{CH} = 6$ and from $\Delta v_{CH} = 6$ to $\Delta v_{CH} = 7$.[17] Similar increases are evident in neopentane-d_9 (Table 2, Figures 2−4). Neopentane-d_6 shows a marked increase from $\Delta v_{CH} = 5$ to $\Delta v_{CH} = 6$ (Table 1, Figures 2−4).

These increases in the fwhm values suggest that through space interactions facilitate stronger coupling between the initially prepared CH pure local mode state and "doorway" states at higher CH stretching amplitudes. However, it is important to note that the classical turning points in Table 12 refer to the direction of extension along the CH bond, and the CH (or CD) bond axes of the proximal hydrogen (or deuterium) atoms on different methyl groups are nearly parallel to one another. Through space coupling would require methyl torsion in combination with high amplitude CH stretching overtone vibrations.

Such through space coupling is less likely in TMS where the longer SiC bond length is reflected in large $r_{HH,space}$ separations. Gas-phase electron diffraction geometries lead to $r_{HH,space}$ values of 305.2 pm[66] and 310 pm.[67] Ab initio determined values of $r_{HH,space}$ are obtained from geometries calculated at B3LYP, B3PW91, and MPW1PW91 levels of theory with a cc-pVDZ basis set and from a geometry calculated at B3LYP/cc-pVTZ. These ab initio values of $r_{HH,space}$ range from 314.2 pm at MPW1PW91/cc-pVDZ to 315.8 pm at B3LYP/cc-pVDZ. In the absence of torsional motion, the separation between the van der Waals surfaces of the nearest hydrogen atoms on different methyl groups ranges from 65 to 76 pm—a substantially larger separation than that in neopentane. Table 12 gives the classical turning points for TMS overtone states, and they are essentially identical to those for neopentane-d_0. Though through space coupling between CH oscillators on different methyl groups might be expected in TMS at excitations above $\Delta v_{CH} = 8$ (classical turning point 75 pm), there is no significant broadening observed in the local modes of TMS through the energy range $\Delta v_{CH} = 3-8$.[17] The $M(CH_3)_4$ homologues tetramethylgermanium and tetramethyltin, both of which have longer MC bond lengths than TMS (and therefore larger $r_{HH,space}$ values), are known to have fwhm values similar to those of TMS for their pure local mode overtone transitions in the range $\Delta v_{CH} = 3-5$.[20]

Evidence for through space interactions in neopentane can also be found through a comparison of the normal mode vibrational frequencies between neopentane and TMS. The two most significant reasons for shifts in vibrational frequency between the two molecules are the increase in mass in going from a central C to a central Si and through space interactions. Vibrational modes 7, 8, 10, 11, 12, and 13 in neopentane-d_0 (Table 5) are significantly higher in frequency than the corresponding modes in TMS (6, 8, 10, 11, 12, and 13, Table 6). However, these modes involve little or no displacement of the central atom. These modes do involve just those nuclear motions that bring the methyl groups into closer proximity, and so are likely to be affected by through space interactions.

Through space interactions can affect IVR in neopentane and TMS in two ways. In general, as noted, they will increase vibrational frequencies because steric crowding creates a barrier to motion. Second, through space interactions increase the mixing of torsional and vibrational states. A comparison of Tables 4 and 5 shows that an increase in normal-mode frequencies will lead to a net increase in possibilities for Fermi resonance in neopentane-d_0. A comparison of Tables 4 and 6 shows that even if through space interaction was significant in TMS, there are fewer modes in TMS that could be moved into a (2:1) resonance through an increase in frequency. Thus the much greater role of through space interaction in neopentane will favor IVR in that molecule over TMS based solely on frequency criteria. However we believe that the greater effect of though space interaction is to promote mixing of torsional and vibrational states,[41,59,60,61] and that this is the dominant source of increased broadening in neopentane relative to TMS for $\Delta v_{CH} > 5$.

Through space coupling can also explain the differences in the $\Delta v_{CH} = 6$ profile of neopentane-d_6 as compared to the profiles of neopentane-d_0 and -d_9. The through space interaction potential is periodic, and changes in the magnitude and periodicity of this potential lead to the mixing of methyl rotor states with vibrational states.[41] If we assume that all CH_3 groups are equally torsionally excited, through space interactions in neopentane-d_0 must have C_{3v} symmetry. Similarly, if all CD_3 groups in neopentane-d_9 are equally torsionally excited, through space interactions will have C_{3v} symmetry. However, the CH_3 and CD_3 groups in neopentane-d_6 will have torsional states with dissimilar populations, and through space interactions will have C_s symmetry. These differences in the symmetries of the through space coupling potential may have an influence on the subtly different profiles at $\Delta v_{CH} = 6$. This may also affect the degree of vibrational state coupling and account for the fact that the significant increase in fwhm occurs in one quantum from $\Delta v_{CH} = 5$ to $\Delta v_{CH} = 6$ in neopentane-d_6 and occurs over two quanta from $\Delta v_{CH} = 5$ through $\Delta v_{CH} = 6$ to $\Delta v_{CH} = 7$ in neopentane-d_0 and -d_9.

Conclusion

Photoacoustic detection of the CH stretching overtone spectra of neopentane-d_0, -d_6, and -d_9 and TMS in the region $\Delta v_{CH} = 4-8$ has revealed broader profiles and more complex structure in the neopentane spectra as compared to TMS. These differences have been ascribed to the relative efficiencies in coupling of pure local mode states $|v, 0, 0\rangle$ with local mode-normal mode combination states $|v - 1, 0, 0\rangle|nv_b\rangle$ and to interactions between methyl torsional and other vibrational modes.

The vibrational frequencies of the normal modes of neopentane-d_0, -d_6, and -d_9 and TMS have been calculated ab initio and scaled with simple empirical scaling factors. The best agreement between calculated and observed frequencies has been obtained at B3LYP/cc-pVDZ for the neopentanes and TMS. Through a comparison of the energies of normal mode states we predicted the occurrence of Fermi resonances in TMS at $\Delta v_{CH} = 4, 5$ and in neopentanes at $\Delta v_{CH} = 4, 5, 7-9$. The frequency data indicated that Fermi resonance is likely to be more efficient in the neopentanes than in TMS because of a greater number of matching states. Torsional−stretching mixing has been shown to be more efficient in neopentane, based, in part, on a more pronounced dependence of local mode parameters $\tilde{\omega}$ and $\tilde{\omega}x$ on the torsional angle ϕ. Nonstationary geometries have been found to affect molecular vibrations and, through modulations in $V(q,\phi)$, appear to preferentially favor IVR in the neopentanes over TMS.

Collision-like interactions between vibrationally excited CH stretching oscillators and adjacent methyl rotors *through space* have been investigated. These through space interactions were found to be greater in the neopentanes than in TMS simply because the CC bond is shorter than the SiC bond. These collision-like interactions were found to augment coupling in the neopentanes relative to TMS by the shifting of vibrational frequencies into a range where more efficient Fermi resonances occur. Additional enhancements in IVR in the neopentanes

relative to TMS have been postulated because of stronger mixing between torsional and vibrational states brought about by stronger through space interactions. Similarity between the $\Delta\upsilon_{CH} = 6$ profiles of neopentane-d_0 and -d_9 and differences with the profile of neopentane-d_6 have been ascribed to differences in the symmetries of their through space coupling potentials.

Acknowledgment. We are grateful to Prof. Ole Sonnich Mortensen for helpful discussions. Funding for this research has been provided by the Natural Sciences and Engineering Council of Canada.

References and Notes

(1) Mecke, R.; Ziegler, R. *Z. Phys.* **1936**, *101*, 405.
(2) Hayward, R. J.; Henry, B. R. *J. Mol. Spectrosc.* **1975**, *57*, 221.
(3) Henry, B. R. *Acc. Chem. Res.* **1977**, *10*, 207.
(4) Watson, I. A.; Henry, B. R.; Ross, I. G. *Spectrochim. Acta A* **1981**, *37*, 857.
(5) Mortensen, O. S.; Henry, B. R.; Mohammadi, M. A. *J. Chem. Phys.* **1981**, *75*, 4800.
(6) Henry, B. R.; Gough, K. M.; Sowa, M. G. *Int. Rev. Phys. Chem.* **1986**, *5*, 133.
(7) Henry, B. R.; Swanton, D. J. *J. Mol. Struct.* **1989**, *202*, 193.
(8) Kjaergaard, H. G.; Proos, R. J.; Turnbull, D. M.; Henry, B. R. *J. Phys. Chem.* **1996**, *100*, 19273.
(9) Sage, M. L.; Jortner, J. *Adv. Chem. Phys.* **1981**, *47*, 293.
(10) Nesbitt, D. J.; Field, R. W. *J. Phys. Chem.* **1996**, *100*, 12735.
(11) Swofford, R. L.; Long, M. E.; Albrecht, A. C. *J. Chem. Phys.* **1976**, *65*, 179.
(12) Henry, B. R. *Acc. Chem. Res.* **1987**, *20*, 429.
(13) Elert, M. L.; Stannard, P. R.; Gelbart, W. M. *J. Chem. Phys.* **1977**, *67*, 5395.
(14) Child, M. S.; Lawton, T. R. *Faraday Discuss. Chem. Soc.* **1981**, *71*, 273.
(15) Henry, B. R.; Tarr, A. W.; Mortensen, O. S.; Murphy, W. F.; Compton, D. A. C. *J. Chem. Phys.* **1983**, *79*, 2583.
(16) Child, M. S.; Halonen, L. *Adv. Chem. Phys.* **1984**, *57*, 1.
(17) Petryk, M. W. P.; Henry, B. R. *Can. J. Chem.* **2001**, *79*, 279.
(18) Tarr, A. W.; Henry, B. R. *J. Chem. Phys.* **1986**, *84*, 1355.
(19) Henry, B. R.; Mohammadi, M. A. *Chem. Phys. Lett.* **1980**, *75*, 99.
(20) Henry, B. R.; Mohammadi, M. A.; Hanazaki, I.; Nakagaki, R. *J. Phys. Chem.* **1983**, *87*, 4827.
(21) Manzanares I, C.; Yamasaki, N. L. S.; Weitz, E.; Knudtson, J. T. *Chem. Phys. Lett.* **1985**, *117*, 477.
(22) Henry, B. R.; Sowa, M. G. *Prog. Anal. Spectrosc.* **1989**, *12*, 349.
(23) Henry, B. R.; Kjaergaard, H. G.; Neifer, B.; Schattka, B. J.; Turnbull, D. M. *Can. J. Appl. Spectrosc.* **1993**, *38*, 42.
(24) Petryk, M. W. P. The Overtone Transitions of Neopentane-d_0, -d_6, -d_9, and Tetramethylsilane. Master's thesis, University of Guelph, 1998.
(25) Morse, P. M. *Phys. Rev.* **1929**, *24*, 57.
(26) Henry, B. R. *The Local Mode Model*. In Vibrational Spectra and Structure, Vol. 10; Durig, J. R., Ed.; Elsevier Scientific: Amsterdam, 1981.
(27) Levine, I. N. *Molecular Spectroscopy*; John Wiley & Sons: New York, 1975.
(28) Zhu, C.; Kjaergaard, H. G.; Henry, B. R. *J. Chem. Phys.* **1997**, *107*, 691.
(29) Kjaergaard, H. G.; Turnbull, D. M.; Henry, B. R. *J. Phys. Chem. A* **1998**, *102*, 6095.
(30) Cavagnat, D.; Lespade, L. *J. Chem. Phys.* **1997**, *106*, 7946.
(31) Cavagnat, D.; Lespade, L. *J. Chem. Phys.* **1998**, *108*, 9275.
(32) Lapouge, C.; Cavagnat, D. *J. Phys. Chem. A* **1998**, *102*, 8393.
(33) Low, G. R.; Kjaergaard, H. G. *J. Chem. Phys.* **1999**, *110*, 9104.
(34) Frisch, M. J.; Trucks, G. W.; Schlegel, H. B.; Scuseria, G. E.; Robb, M. A.; Cheeseman, J. R.; Zakrzewski, V. G.; Montgomery, J. A., Jr.; Stratmann, R. E.; Burant, J. C.; Dapprich, S.; Millam, J. M.; Daniels, A. D.; Kudin, K. N.; Strain, M. C.; Farkas, O.; Tomasi, J.; Barone, V.; Cossi, M.; Cammi, R.; Mennucci, B.; Pomelli, C.; Adamo, C.; Clifford, S.; Ochterski, J.; Petersson, G. A.; Ayala, P. Y.; Cui, Q.; Morokuma, K.; Malick, D. K.; Rabuck, A. D.; Raghavachari, K.; Foresman, J. B.; Cioslowski, J.; Ortiz, J. V.; Stefanov, B. B.; Liu, G.; Liashenko, A.; Piskorz, P.; Komaromi, I.; Gomperts, R.; Martin, R. L.; Fux, D. J.; Keith, T.; Al-Laham, M. A.; Peng, C. Y.; Nanayakkara, A.; Gonzalez, C.; Challacombe, M.; Gill, P. M. W.; Johnson, B.; Chen, W.; Wong, M. W.; Andres, J. L.; Gonzalez, C.; Head-Gordon, M.; Replogle, E. S. *Gaussian 98*, Revision A.5; Gaussian Inc.: Pittsburgh, PA, 1998.
(35) Ochterski, J. W. Vibrational Analysis in *Gaussian*. Technical Report; Gaussian, Inc.: Carnegie Office Park, Building 6, Suite 230 Carnegie, PA 15106, 1999. This publication is available via the worldwide web at http://www.Gaussian.com/vib.htm.
(36) SpectraCalc is commercially available software from Galactic Industries Corp.
(37) Sibert, E. L., III; Hynes, J. T.; Reinhardt, W. P. *J. Chem. Phys.* **1984**, *81*, 1135.
(38) Sibert, E. L., III.; Reinhardt, W. P.; Hynes, J. T. *J. Chem. Phys.* **1984**, *81*, 1115.
(39) Quack, M. *J. Mol. Struct.* **1993**, *292*, 171.
(40) Sowa, M. G.; Henry, B. R. *J. Chem. Phys.* **1991**, *95*, 3040.
(41) Moss, D. B.; Parmenter, C. S.; Ewing, G. E. *J. Chem. Phys.* **1987**, *86*, 51.
(42) Rauhut, G.; Pulay, P. *J. Phys. Chem.* **1995**, *99*, 3093.
(43) Baker, J.; Jarzecki, A. A.; Pulay, P. *J. Phys. Chem. A* **1998**, *102*, 1412.
(44) Magdó, I.; Németh, K.; Mark, F.; Hildebrandt, P.; Schaffner, K. *J. Phys. Chem. A* **1999**, *103*, 289.
(45) Becke, A. D. *J. Chem. Phys.* **1993**, *98*, 5648.
(46) Raymond, K. S.; Wheeler, R. A. *J. Comput. Chem.* **1999**, *20*, 207.
(47) Lee, C.; Yang, W.; Parr, R. G. *Phys. Rev. B* **1988**, *37*, 785.
(48) Miehlich, B.; Savin, A.; Stoll, H.; Preuss, H. *Chem. Phys. Lett.* **1989**, *157*, 200.
(49) Dunning, T. H., Jr. *J. Chem. Phys.* **1989**, *90*, 1007.
(50) Zarkova, L.; Pirgov, P.; Hohm, U.; Chrissanthopoulos, A.; Stefanov, B. B. *Int. J. Thermophys.* **2000**, *21*, 1439.
(51) Kjaergaard, H. G.; Turnbull, D. M.; Henry, B. R. *J. Chem. Phys.* **1993**, *99*, 9438.
(52) Palmö, K.; Mirkin, N. G.; Krimm, S. *J. Phys. Chem. A* **1998**, *102*, 6448.
(53) Allen, W. D.; Császár, A. G. *J. Chem. Phys.* **1993**, *98*, 2983.
(54) Allen, W. D.; East, A. L. L.; Császár, A. G. *Ab Initio Anharmonic Vibrational Analyses of Non-Rigid Molecules*; In Structures and Conformations of Non-Rigid Molecules, Vol. 410; Laane, J., Dakkouri, M., van der Veken, B., Oberhammer, H., Eds.; Kluwer Academic Publishers: Dordrecht, The Netherlands, 1993.
(55) Kjaergaard, H. G.; Rong, Z.; McAlees, A. J.; Howard, D. L.; Henry, B. R. *J. Phys. Chem. A* **2000**, *104*, 6398.
(56) Lespade, L.; Cavagnat, D.; Rodin-Bercion, S. *J. Phys. Chem. A* **2000**, *104*, 9880.
(57) Bellamy, L. J. *The Infrared Spectra of Complex Molecules. Advances in Infrared Group Frequencies*, 2nd ed.; Chapman and Hall: London and New York, 1980.
(58) Horák, M.; Plıva, J. *Collect. Czech. Chem. Commun.* **1960**, *25*, 1679.
(59) Martens, C. C.; Reinhardt, W. P. *J. Chem. Phys.* **1990**, *93*, 5621.
(60) Tan, X.-Q.; Majewski, W. A.; Plusquellic, D. F.; Pratt, D. W. *J. Chem. Phys.* **1991**, *94*, 7721.
(61) Lu, K.-T.; Weinhold, F.; Weisshaar, J. C. *J. Chem. Phys.* **1995**, *102*, 6787.
(62) Turnbull, D. M.; Kjaergaard, H. G.; Henry, B. R. *Chem. Phys.* **1995**, *195*, 129.
(63) Beagley, B.; Brown, D. P.; Monaghan, J. J. *J. Mol. Struct.* **1969**, *4*, 233.
(64) Bartell, L. S.; Bradford, W. F. *J. Mol. Struct.* **1977**, *37*, 113.
(65) Pauling, L. *The Nature of the Chemical Bond*, 3rd ed.; Cornell University Press: Ithaca, NY, 1960.
(66) Beagley, B.; Monaghan, J. J.; Hewitt, T. G. *J. Mol. Struct.* **1971**, *8*, 401.
(67) Sheehan, W. F., Jr.; Schomaker, V. *J. Am. Chem. Soc.* **1952**, *74*, 3956.
(68) Sverdlov, L. M.; Kovner, M. A.; Krainov, E. P. *Vibrational Spectra of Polyatomic Molecules*; John Wiley & Sons: New York, 1974; translated from Russian by IPST Staff.
(69) Sportouch, S.; Lacoste, C.; Gaufrès, R. *J. Mol. Struct.* **1971**, *9*, 119.